RESEARCH ARTICLE

Structural relaxation dynamics of a silicate glass probed by refractive index and ionic conductivity

Ricardo Felipe Lancelotti[1,2] | **Ana Candida Martins Rodrigues**[2] |
Edgar Dutra Zanotto[2]

[1]Graduate Program in Materials Science and Engineering, Federal University of São Carlos, São Carlos, SP, Brazil

[2]Center for Research, Technology and Education in Vitreous Materials, Department of Materials Engineering, Federal University of São Carlos, São Carlos, SP, Brazil

Correspondence
Ricardo Felipe Lancelotti, Federal University of São Carlos, Department of Materials Engineering, Vitreous Materials Laboratory, 13565-905 São Carlos, SP, Brazil.
Email: lancelotti.r@dema.ufscar.br

Editor's Choice
The Editor-in-Chief recommends this outstanding article.

Abstract
Relaxation occurs spontaneously in all glasses and is a fundamental step of important technological processes, such as annealing, crystal nucleation, and chemical strengthening by ion exchange. Despite extensive studies over the past decades, there are still conflicting results on whether the kinetics of structural relaxation depends on the analyzed property. Thus, in this study, we used a lithium disilicate glass as a model composition to determine the structural relaxation kinetics during physical aging experiments by measuring the time evolution of the refractive index and ionic conductivity down to 35 K below the initial fictive temperature. In all cases, variations in these properties were adequate to capture the structural changes throughout the aging experiments. At each temperature, the experimental relaxation data fit quite well with the classical stretched exponential relation. We also found that the relaxation process starts faster when probed by ionic conductivity than by refractive index; however, they show similar average relaxation times. These very small structural rearrangements are always the same, but ionic conductivity changes faster than refractive index at the beginning of the process. Our comprehensive results strongly indicate that relaxation dynamics is indeed dependent on the analyzed property.

KEYWORDS
aging, fictive temperature, glass, ionic conductivity, lithium disilicate, refractive index, structural relaxation

1 | INTRODUCTION

Glasses are noncrystalline, thermodynamically unstable materials that spontaneously relax toward the supercooled liquid (SCL) state.[1] Structural relaxation is defined as the structural rearrangement of a material over time in the absence of stress. Relaxation times vary from seconds in the glass transition region to geological times at room temperature[2,3] and are crucial during heat treatment, strongly influencing key processes of glasses, such as residual stress relief,[4] crystal nucleation,[5,6] and chemical strengthening.[7,8]

Structural relaxation is a spontaneous phenomenon that depends on the temperature, pressure, chemical composition, and thermobaric history of the glass. It is the change of the glass structure from a thermodynamically unstable state with an initial fictive temperature (T_f) and fictive pressure (p_f) toward a metastable equilibrium, reaching once again the SCL state at the investigated temperature or pressure. Thus, all glass properties

depend on its thermobaric history. Furthermore, knowledge about this dependence is key to optimizing the processing conditions of glasses to obtain the desired properties.[9]

Relaxation—also known as aging—experiments may be followed through measurement over time of certain properties, for example, viscosity,[10] refractive index,[11] density,[12] ionic conductivity,[13] enthalpy,[14] or thermal expansion coefficient,[15] among others. These experiments are quite challenging when performed well below the glass transition region because of the long times involved, which can exceed the typical laboratory time scales.[16] At low temperatures, experiments may be continued for months and even years.[17] Therefore, most experimental works focus on temperature intervals that are not far below the glass transition region.

Such a slow process is normally attributed to the so-called primary or α-relaxation, which involves a cooperative motion of the structural units.[18] The secondary or β-relaxation, also known as the Johari–Goldstein relaxation,[19] refers to faster, non-collective motion, which involves the local motion of loosely packed regions[20] that occur on the order of 10^{-5} s.[21] β-relaxation is sometimes divided into two types, slow and fast, because there are different sizes of local motion, as shown for metallic glasses,[22,23] in which very fast relaxation is initiated and centered in some local sites. In contrast, slow relaxation spreads out to the surroundings, including to less-mobile atoms. All these relaxation types become indistinguishable at high temperatures because all structural rearrangements are accessible in a short period.

The time dependence of a relaxing property at constant pressure and temperature is often described by a stretched exponential behavior, which can be derived from a collective average of exponential decay with different time constants resulting from density and composition fluctuations in the glass.[24] The empirical Kohlrausch equation,[25,26] which is also known as the Kohlrausch–Williams–Watts function[27] or stretched exponential,[28] has been successfully used to analyze the structural relaxation kinetics of glasses and is expressed as

$$\phi\,(t) = \exp\left[-\left(\frac{t}{\tau_k}\right)^{\beta}\right], \tag{1}$$

where ϕ is the relaxation parameter, τ_k is the characteristic relaxation time, t is the experimental time, and β is the Kohlrausch or stretching exponent—a parameter that specifies the distribution width of the relaxation times. The average relaxation time, $\langle\tau\rangle$, for stretched exponential relaxation is defined as the area under the curve $\phi(t)$ given

by

$$\langle\tau\rangle = \int\limits_{0}^{\infty} \phi\,(t)\,dt = \frac{\tau_k}{\beta}\,\Gamma\left(\frac{1}{\beta}\right). \tag{2}$$

Equation (1) becomes a true exponential for $\beta = 1$. Normally, β decreases with decreasing the temperature. Lower values imply a wider distribution of relaxation times, that is, structural units with different relaxation times. Figure 1 illustrates the behavior of the relaxation parameter as a function of time for different values of the stretching exponent. The curves intersect at the same point when $t = \tau_k$ (10 s in this example). Thus, $\phi = \exp(-1) \approx 0.368$, that is, the characteristic relaxation time occurs for a 63.2% relaxed material.

Property relaxation during a step change from a temperature (T_a) to another temperature (T_b) may be defined as[29]

$$\phi\,(t) = \frac{p\,(t) - p_\infty}{p_0 - p_\infty} = \frac{T_f\,(t) - T_b}{T_a - T_b}, \tag{3}$$

where p is the property value, p_∞ is the equilibrium value of that property at T_b, p_0 is the property value at the initial temperature T_a, and T_f is the fictive temperature, which changes from T_a to T_b during relaxation. This expression assumes that the initial fictive temperature is T_a, which can be preestablished by previous annealing of the glass at T_a.

Combining Equations (1) and (3) yields the stretched exponential relation, the following equation, which provides an excellent fit to a wide variety of isothermal
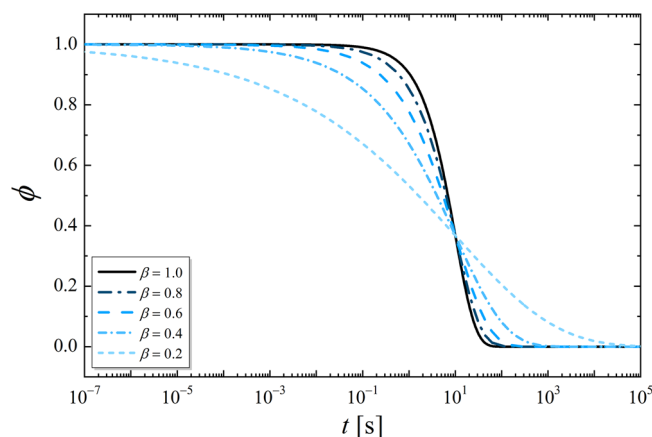
FIGURE 1 Relaxation parameter as a function of time, calculated for $\tau_k = 10$ s and different stretching exponent values. It is important to note the extremely wide time scale spanning several orders of magnitude.

structural relaxation data[5,6,13,30–33]:

$$p\ (t) = p_\infty + (p_0 - p_\infty)\exp\left[-\left(\frac{t}{\tau_k}\right)^\beta\right]. \qquad (4)$$

A dependence of the relaxation dynamics on the actual property being measured has been studied by many authors; however, the current situation is still controversial: although some researchers advocate that the relaxation dynamics is the same for different properties, others sustain that it is different.

For instance, DeBolt et al.[14] compared their enthalpy (H) relaxation data of B_2O_3 glass at 536.4 K with the Boesch et al.[34] refractive index (n) relaxation data for the same glass composition and temperature and found that enthalpy relaxes faster than refractive index. In a classic paper, Moynihan et al.[35] summarized the kinetic parameters of the structural relaxation process of several authors and materials and concluded that the average relaxation time and the stretching exponent are different for different properties of the same glass. Although those authors compared some properties for the same temperature and nominal glass composition, the measurements were performed by different research groups using glass samples of different batches, which were produced and measured in different environments. Hence, because of the likely difference in impurity contents, especially water, which strongly affects relaxation dynamics, this comparison is subject to significant uncertainty. However, an aging study conducted by Sasabe and Moynihan[36] compared the enthalpy and dielectric relaxation results of samples from the same batch of poly(vinyl acetate) above the glass transition region. They also found that enthalpy and dielectric relaxation measured at the same temperature seemed to be characterized by somewhat different relaxation times. Moreover, Dingwell and Webb[37] compiled relaxation times in $Na_2Si_3O_7$ melt from shear viscosity and electrical relaxation data. As expected, they showed that the relaxation times estimated from electrical modulus are much faster than those from shear viscosity. Therefore, these four studies indicated significant differences in relaxation dynamics probed by distinct properties.

On the other hand, Rekhson et al.[38] analyzed a window glass and reported that volume and viscosity relax with similar kinetics within the experimental uncertainty. Webb et al.[15] concluded that relaxation times for shear viscosity, volume, and enthalpy are equivalent in $Na_2Si_2O_5$. Moreover, Echeverría et al.[39] investigated the relaxation behavior of amorphous selenium through enthalpy recovery and the creep-recovery response. They found that the times to reach equilibrium seem to be the same in the glass transition region, but to diverge at lower temperatures, with enthalpy coming to equilibrium before volume and creep. Málek et al.[40] also used amorphous selenium to study the specific volume and enthalpy relaxation in the glass transition region. Their relaxation parameters were only slightly different, and they concluded that these two properties relax with the same kinetics.

Hence, the objective of this work is to verify this controversy by systematically comparing the structural relaxation dynamics throughout the physical aging of a lithium disilicate (LS_2) glass through changes in refractive index (n) and ionic conductivity (σ) at several temperatures below the initial T_f. In this case, these two properties were measured in glass samples from the same batch, treated at identical conditions.

2 | MATERIALS AND METHODS

Lithium disilicate ($Li_2Si_2O_5$, LS_2), which is a model glass for crystallization studies, was chosen for this study. This glass was used recently to clarify the effect of structural relaxation on crystal nucleation.[5] The LS_2 glass samples used in this work are from the same batch as those used by Cassar et al.[41] in an investigation about the classical nucleation theory. The glass was prepared by the traditional melting and quenching methods using ground quartz SiO_2 (Vitrovita, Brazil, 99.9%) and Li_2CO_3 (Alfa Aesar, USA, 99.0%). It was annealed at 663 K for 2 h followed by slow cooling to room temperature at 3 K min^{-1} to alleviate the residual stresses and allow sample preparation. The laboratory glass transition temperature, T_g, of the annealed glass was 727 K, measured by differential scanning calorimetry (DSC 404, Netzsch) at a heating rate of 10 K min^{-1}. This determination was necessary to identify the heat treatment temperatures required and define an initial fictive temperature, T_f, of the physical aging experiments.

The samples were divided into two sets so that glasses with two different initial fictive temperatures could be obtained. The first set was treated at 720 K (T_{f1}) and the second set at 727 K (T_{f2}), both for 4 h, which is sufficient to reach their metastable SCL equilibrium state (>99% relaxed). Subsequently, physical aging experiments were conducted by alternating isothermal treatments at $T < T_f$, with determinations of refractive index at room temperature and ionic conductivity at 308 K. To this end, the samples were submitted to isothermal treatments at different temperatures (705, 695, and 685 K), which are 15, 25, and 35 K below T_{f1}, and at 703 K, which is 24 K below T_{f2}, for cumulative times, that is, the samples were heat-treated at the indicated temperature, taken out of the furnace, had their proprieties measured, and were inserted back into the furnace at the study temperature until a constant value within the experimental error was reached. The experimental data were fitted with Equation (4), which

was able to describe quite well the individual isothermal structural relaxation kinetics. The confidence bands were calculated considering two standard deviations.

The refractive index measurements were repeated 10 times at room temperature using a high-precision refractometer (Pulfrich PR2, Carl Zeiss) with a mercury lamp in a monochromatic green e-line, $\lambda = 546.1$ nm, and a VoF5 prism, $n_{546.1,p} = 1.74800(1)$. The 10 mm × 10 mm × 3 mm samples had two perpendicular polished faces. The refractive index, n_λ, measurement is based on the deviation angle of the refracted beam (γ), which is given by the following equation:

$$n_\lambda = \sqrt{n_{\lambda,p}^2 - \cos(\gamma)} \sqrt{n_{\lambda,p}^2 - \cos^2(\gamma)}. \quad (5)$$

The electrical conductivity measurements were performed at 308 K by impedance spectroscopy using a high-performance impedance analyzer (Alpha-A, Novocontrol) in a frequency range from 10 MHz to 0.1 Hz and a voltage amplitude of 300 mV. The two samples used had two parallel surfaces with thickness and area values of $l_1 = 0.2875(5)$ cm and $S_1 = 0.696(2)$ cm^2, and $l_2 = 0.3185(5)$ cm and $S_2 = 0.902(1)$ cm^2, respectively. Before the measurements, gold electrodes were sputtered on the two parallel surfaces using a sputter (Q150R ES, Quorum) with the current of 20 mA and time deposition of 300 s. Impedance data can be represented in several correlated formalisms, including the impedance complex plane plot with the imaginary part of impedance $-Z''$ at the y-axis and the real part Z' at the x-axis. Sample resistance (R) can be directly read at the low-frequency intersection of the semicircle with the real x-axis. Thus, the ionic conductivity, σ, is calculated by the following equation:

$$\sigma = \frac{1}{R}\frac{l}{S}. \quad (6)$$

3 | RESULTS AND DISCUSSION

Figure 2 shows the temporal evolution of the refractive index and ionic conductivity during the isothermal heat treatments at 705, 703, 695, and 685 K of LS$_2$ samples pre-annealed at 720 and 727 K. The refractive index and ionic conductivity data for each treatment time and temperature are provided in Tables S1–S6.

The magnitude of property changes associated with completing relaxation increased as the study temperature moved away from the initial T_f toward lower temperatures, corroborating previous results for other glasses via refractive index[6,33,42] and ionic conductivity.[13] Figure 3 shows the complex impedance plots measured at 308 K for a
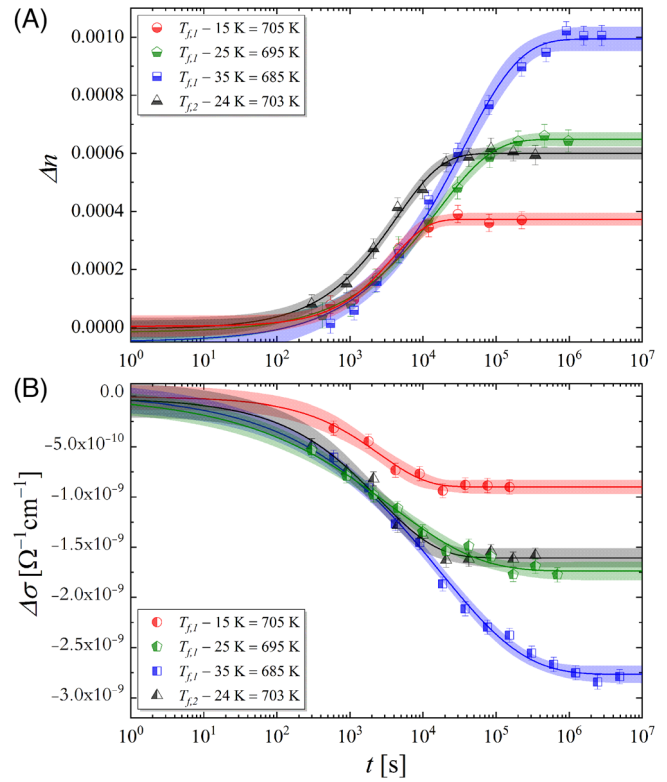

FIGURE 2 Variation of (A) refractive index and (B) ionic conductivity of an LS$_2$ glass as a function of heat treatment time for four physical aging experiments below a pre-established initial T_f. The solid lines are the stretched exponential relation regressions, and the shaded areas show the confidence bands.
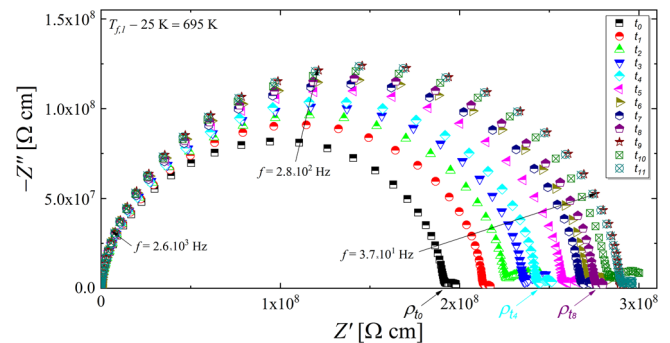
FIGURE 3 Complex impedance plots measured at 308 K for a sample ($l/S = 0.413$ cm^{-1}) heat-treated at $T_{f1} - 25$ K = 695 K by $t_0 = 0$ s, $t_1 = 300$ s, $t_2 = 900$ s, $t_3 = 2100$ s, $t_4 = 4500$ s, $t_5 = 9900$ s, $t_6 = 20\,700$ s, $t_7 = 42\,300$ s, $t_8 = 85\,500$ s, $t_9 = 171\,900$ s, $t_{10} = 344\,700$ s, and $t_{11} = 690\,300$ s.

sample aged at $T_{f1} - 25$ K for different times—the plots for other aging temperatures are provided in Figures S1–S3. It is important to emphasize that, unlike some authors,[37,43,44] we did not measure the electrical relaxation, which leads to a very fast relaxation behavior. Instead, the inverse of ionic conductivity (ionic resistivity, ρ) was promptly read at the low-frequency intersection of the semicircle with the
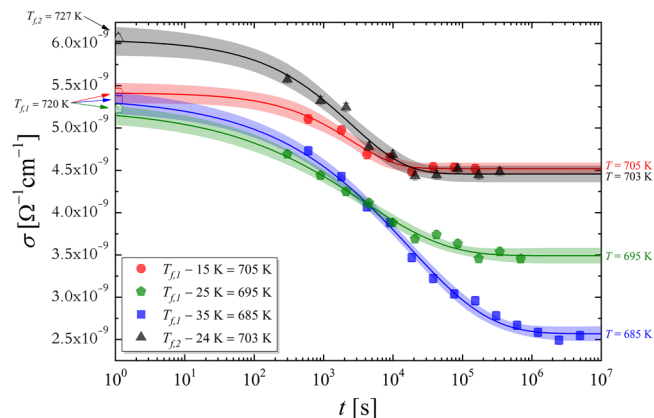
FIGURE 4 Temporal evolution of ionic conductivity measured at 308 K of an LS$_2$ glass during aging at different temperatures. The open symbols refer to the values of ionic conductivity measured at $t = 0$ s, that is, the values for the initial T_f.

x-axis, because the impedance results were normalized by the geometrical factor of the sample (l/S, respectively, sample thickness and area). The temporal changes were then fitted by the stretched exponential relation (Equation 4).

Property variations are strongly linked to the difference between the initial T_f and the measurement temperature, for example, there is a similar variation when the property is measured at $T_{f1} - 25$ K and $T_{f2} - 24$ K (see Figure 2), although the initial fictive temperatures and also the studied temperatures were different. Figure 4 illustrates this behavior produced by two different initial fictive temperatures (720 and 727 K) for ionic conductivity data; the samples were heat-treated at different temperatures (685, 695, 703, and 705 K) for cumulative times and measured at 308 K. Such temporal changes measured by refractive index and ionic conductivity were fitted by the stretched exponential relation, which described quite well all the experimental data. Figure 5 shows the adjustable parameters ($p_\infty - p_0$, τ_k, and β) obtained from regressions, as well as the average relaxation time, $\langle \tau \rangle$. Linear regression analyses were performed considering one standard deviation.

The results shown in Figure 5 indicate a relationship between each parameter and the temperature. The difference $p_\infty - p_0$ is zero for $T = T_f$. When the difference between the T_f and the study temperature increases in the $T < T_f$ range, $n_\infty - n_0$ also increases, whereas $\sigma_\infty - \sigma_0$ and β decrease, and τ_k and $\langle \tau \rangle$ increase exponentially. These results agree with those previously reported for a lead metasilicate glass via changes in refractive index.[33]

Figure 6 shows the relaxation parameter, ϕ, as a function of time. The ionic conductivity undergoes a faster start of relaxation, which yields a lower characteristic relaxation time, as shown in Figure 5C. Ionic conductivity also has the lower stretching exponent, Figure 5B.

Equation (2) demonstrates that these two parameters have distinct effects on $\langle \tau \rangle$, resulting in a very similar average relaxation time for both properties. The aging results at $T_{f1} - 35$ K, shown in Figure 6C, have the larger change in T_f and, consequently, larger property variations and lower uncertainty.

We would like to draw the reader's attention to the behavior of these properties. Ionic conductivity changes faster at the beginning of the process and has a lower stretching exponent than refractive index, but they show similar average relaxation times. The stretching exponent is a measure of the width of the relaxation dynamics, encompassing the slowest to the fastest structural groups in the α-relaxation and the so-called slow β-relaxation (as opposed to fast β-relaxation). In other words, the characteristic relaxation time and the stretching exponent resulting from conductivity measurements are *shorter* than those obtained from refractive index; however, the average relaxation times are similar.

We have shown that it is not straightforward to classify the relaxation type as α- or slow β-relaxation via different properties. Indeed, ionic conductivity was measured by the migration of lithium ions in the LS$_2$ glass, but this process becomes easier or more difficult by the cooperative relaxation of the lattice depending on whether the ionic conductivity is measured above or below the fictive temperature.[13] Moreover, as shown in Figure 5, the stretching exponent is a function of both temperature and thermal history and decreases as the temperature moves away from the initial T_f toward lower temperatures. This result agrees with other experimental findings.[33,45]

Lower stretching exponents result from relaxation at lower temperatures as well as from some properties such as ionic conductivity, whereas the refractive index yields larger stretching exponents. Consequently, it is possible to distinguish different kinetics in the same sample by measuring different properties at a given temperature. Recently, the temperature dependence of the stretching exponent has been discussed.[46,47] It is sometimes assumed that β is a constant of 3/5 or 3/7, as derived by Phillips[48,49] and experimentally indicated by other authors,[50,51] or that it is only temperature dependent.[45] The current results showed herein evidence that the stretching exponent indeed depends on the measurement temperature, the fictive temperature, and also on the analyzed property, that is, $\beta(T, T_f, p)$.

Summarizing, the most relevant result of this work is that the measured structural relaxation kinetics depends on the analyzed property, which corroborates the findings of some previous studies.[14,34–36] The dependence of relaxation dynamics on the measured property may be explained by the different effects that structural rearrangements of the glass have on each property.
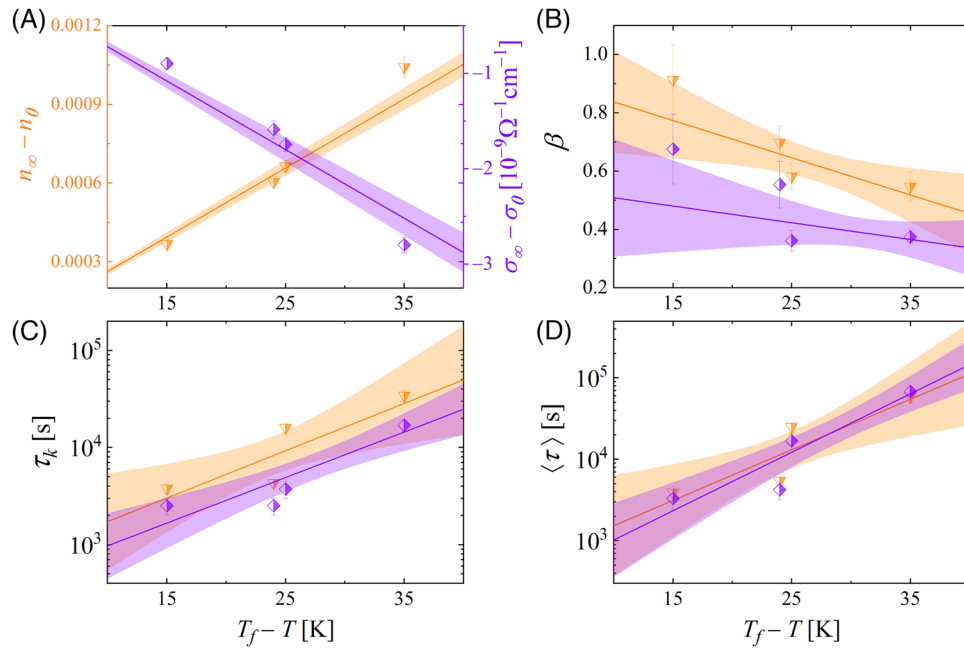
FIGURE 5 Parameters related to the relaxation of refractive index (orange triangles) and ionic conductivity (violet diamonds): (A) variation of properties, (B) stretching exponent, (C) characteristic relaxation time, and (D) average relaxation time. The shaded areas show the confidence bands.
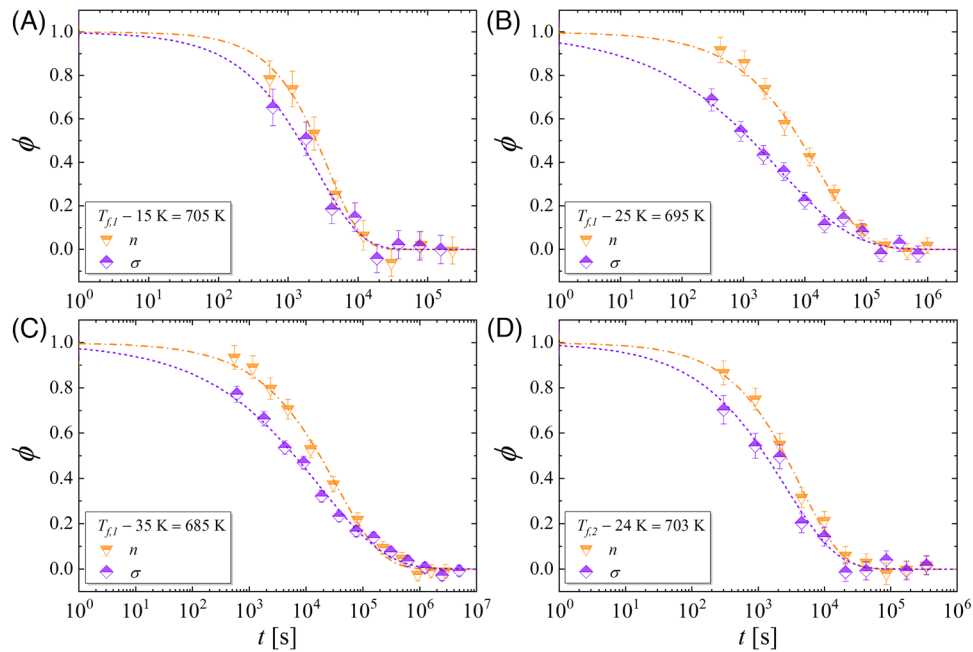
FIGURE 6 Relaxation parameter as a function of heat treatment time calculated by the variation of the refractive index and ionic conductivity at (A) $T_{f,1} - 15$ K, (B) $T_{f,1} - 25$ K, (C) $T_{f,1} - 35$ K, and (D) $T_{f,2} - 24$ K.

These rearrangements increase the glass density when the study temperature is lower than the initial fictive temperature[12,52] and change the local environment of the lithium ions.[53] Thus, changes in density may have a greater influence on the refractive index, whereas the ionic conductivity may be more influenced in the early stages by changes in the distance of lithium ions, although it is also affected by changes in density. The structural changes are

always the same, but small structural rearrangements at the beginning of the process imply more marked changes in ionic conductivity than in refractive index.

4 | CONCLUSIONS

We measured the structural relaxation kinetics throughout the physical aging of a lithium disilicate glass by changes in refractive index and ionic conductivity below the initial fictive temperature. At all temperatures, the property variations were precise enough to capture the structural changes during the relaxation process. The classical stretched exponential relation describes quite well all the isothermal experimental relaxation data during aging. The results confirmed that the stretching exponent is indeed a complex parameter, because it is a strong function of the measurement temperature, fictive temperature, and analyzed property.

The relaxation process starts faster when measured by ionic conductivity than by refractive index. Ionic conductivity also shows a lower stretching exponent than refractive index; however, both properties present similar average relaxation times. This means that the very small structural rearrangements that occur at the beginning of glass relaxation have a greater influence on ionic conductivity, whereas refractive index is more influenced by the more cooperative α-relaxation. As a result, the relaxation kinetics measured for the same glass in the same condition indeed depends on the analyzed property. This result is not surprising, but sheds light on the controversy within the glass research community.

ORCID
Ricardo Felipe Lancelotti https://orcid.org/0000-0002-6111-6520
Ana Candida Martins Rodrigues https://orcid.org/0000-0003-1689-796X
Edgar Dutra Zanotto https://orcid.org/0000-0003-4931-4505

REFERENCES
1. Zanotto ED, Mauro JC. The glassy state of matter: its definition and ultimate fate. J Non-Cryst Solids. 2017;471:490–5.
2. Zanotto ED, Gupta PK. Do cathedral glasses flow?—Additional remarks. Am J Phys. 1999;67(3):260–2.
3. Gulbiten O, Mauro JC, Guo X, Boratav ON. Viscous flow of medieval cathedral glass. J Am Ceram Soc. 2018;101:5–11.
4. Tool AQ. Relaxation of stresses in annealing glass. J Res Nat Bur Stand (US). 1945;34(2):199–211.
5. Fokin VM, Abyzov AS, Yuritsyn NS, Schmelzer JWP, Zanotto ED. Effect of structural relaxation on crystal nucleation in glasses. Acta Mater. 2021;203:116472.
6. Rodrigues LR, Abyzov AS, Fokin VM, Zanotto ED. Effect of structural relaxation on crystal nucleation in a soda-lime-silica glass. J Am Ceram Soc. 2021;104(7):3212–23.
7. Varshneya AK. Chemical strengthening of glass: lessons learned and yet to be learned. Int J Appl Glass Sci. 2010;1(2):131–42.
8. Varshneya AK, Olson GA, Kreski PK, Gupta PK. Buildup and relaxation of stress in chemically strengthened glass. J Non-Cryst Solids. 2015;427:91–7.
9. Yuan B, Chen H, Sen S. Aging-induced structural evolution of a GeSe$_2$ glass network: the role of homopolar bonds. J Phys Chem B. 2022;126(4):946–52.
10. Lillie HR. Viscosity-time-temperature relations in glass at annealing temperatures. J Am Ceram Soc. 1933;16(12):619–31.
11. Winter A. Transformation region of glass. J Am Ceram Soc. 1943;26(6):189–200.
12. Ritland HN. Density phenomena in the transformation range of a borosilicate crown glass. J Am Ceram Soc. 1954;37(8):370–7.
13. Bragatto CB, Cassar DR, Peitl O, Souquet J-L, Rodrigues ACM. Structural relaxation in AgPO$_3$ glass followed by in situ ionic conductivity measurements. J Non-Cryst Solids. 2016;437:43–7.
14. DeBolt MA, Easteal AJ, Macedo PB, Moynihan CT. Analysis of structural relaxation in glass using rate heating data. J Am Ceram Soc. 1976;59(1–2):16–21.
15. Webb SL. Shear, volume, enthalpy and structural relaxation in silicate melts. Chem Geol. 1992;96(3–4):449–57.
16. Berthier L, Ediger MD. How to "measure" a structural relaxation time that is too long to be measured? J Chem Phys. 2020;153(4):44501.
17. Micoulaut M. Relaxation and physical aging in network glasses: a review. Rep Prog Phys. 2016;79(6):66504.
18. Ngai KL. Correlation between the secondary β-relaxation time at Tg with the Kohlrausch exponent of the primary α relaxation or the fragility of glass-forming materials. Phys Rev E. 1998;57(6):7346.
19. Johari GP, Goldstein M. Viscous liquids and the glass transition. II. Secondary relaxations in glasses of rigid molecules. J Chem Phys. 1970;53(6):2372–88.
20. Mangion MBM, Johari GP. Relaxations of thermosets. III. Sub-Tg dielectric relaxations of bisphenol-A–based epoxide cured with different cross-linking agents. J Polym Sci, B: Polym Phys. 1990;28(1):71–83.
21. Varshneya AK, Mauro JC. Fundamentals of inorganic glasses. 3rd ed. Sheffield: Elsevier; 2019.
22. Wang Q, Zhang ST, Yang Y, Dong YD, Liu CT, Lu J. Unusual fast secondary relaxation in metallic glass. Nat Commun. 2015;6(1):7876.
23. Wang Z, Wang W-H. Flow units as dynamic defects in metallic glassy materials. Natl Sci Rev. 2019;6(2):304–23.
24. Greaves GN, Sen S. Inorganic glasses, glass-forming liquids and amorphizing solids. Adv Phys. 2007;56(1):1–166.

25. Kohlrausch R. Theorie des elektrischen Rückstandes in der Leidener Flasche. Ann Phys. 1854;167(2):179–214.

26. Kohlrausch F. Ueber die elastische Nachwirkung bei der Torsion. Ann Phys. 1863;195(7):337–68.

27. Williams G, Watts DC. Non-symmetrical dielectric relaxation behaviour arising from a simple empirical decay function. Trans Faraday Soc. 1970;66:80–5.

28. Chamberlin RV, Mozurkewich G, Orbach R. Time decay of the remanent magnetization in spin-glasses. Phys Rev Lett. 1984;52(10):867.

29. Narayanaswamy OS. A model of structural relaxation in glass. J Am Ceram Soc. 1971;54(10):491–8.

30. Malfait WJ, Halter WE. Structural relaxation in silicate glasses and melts: high-temperature Raman spectroscopy. Phys Rev B. 2008;77(1):14201.

31. Bokov NA, Golubkov VV. Temperature dependences of the density of borate glasses in equilibrium states at temperatures below the glass transition point. Glass Phys Chem. 2008;34(5):527–33.

32. Duan F, Pan J, Lin Y, Li Y. Significant structural relaxation in a Mo-O binary amorphous alloy. J Non-Cryst Solids. 2019;514:10–4.

33. Lancelotti RF, Cassar DR, Nalin M, Peitl O, Zanotto ED. Is the structural relaxation of glasses controlled by equilibrium shear viscosity? J Am Ceram Soc. 2021;104(5):2066–76.

34. Boesch L, Napolitano A, Macedo PB. Spectrum of volume relaxation times in B_2O_3. J Am Ceram Soc. 1970;53(3):148–53.

35. Moynihan CT, Macedo PB, Montrose CJ, Montrose CJ, Gupta PK, DeBolt MA, et al. Structural relaxation in vitreous materials. Ann NY Acad Sci. 1976;279(1):15–35.

36. Sasabe H, Moynihan CT. Structural relaxation in poly(vinyl acetate). J Polym Sci Polym Phys Ed. 1978;16(8):1447–57.

37. Dingwell DB, Webb SL. Relaxation in silicate melts. Eur J Mineral. 1990;2(2):427–49.

38. Rekhson SM, Bulaeva A V, Mazurin OV. Changes in the linear dimensions and viscosity of window glass during stabilization. Inorg Mater. 1971;7(4):622–3.

39. Echeverría I, Kolek PL, Plazek DJ, Simon SL. Enthalpy recovery, creep and creep–recovery measurements during physical aging of amorphous selenium. J Non-Cryst Solids. 2003;324(3):242–55.

40. Málek J, Svoboda R, Pustková P, Čičmanec P. Volume and enthalpy relaxation of a-Se in the glass transition region. J Non-Cryst Solids. 2009;355:264–72.

41. Cassar DR, Serra AH, Peitl O, Zanotto ED. Critical assessment of the alleged failure of the Classical Nucleation Theory at low temperatures. J Non-Cryst Solids. 2020;547:120297.

42. Spinner S, Napolitano A. Further studies in the annealing of a borosilicate glass. J Res Natl Bur Stand A Phys Chem. 1966;70:147–52.

43. Howell FS, Bose RA, Macedo PB, Moynihan CT. Electrical relaxation in a glass-forming molten salt. J Phys Chem. 1974;78(6):639–48.

44. Kumar KN, Kostrzewa M, Ingram A, Suresh B, Reddy ASS, Gandhi Y, et al. Dielectric features, relaxation dynamics and a.c. conductivity studies on Ag^+ mixed lead arsenate glass ceramics. J Mater Sci: Mater Electron. 2018;29:1153–72.

45. Ngai KL. Relaxation and diffusion in complex systems. New York: Springer Science+Business Media; 2011. p. 835.

46. Wilkinson CJ, Doss K, Gulbiten O, Allan DC, Mauro JC. Fragility and temperature dependence of stretched exponential relaxation in glass-forming systems. J Am Ceram Soc. 2021;104(9):4559–67.

47. Hauke BM, Mancini M, Mauro JC. Impact of a temperature-dependent stretching exponent on glass relaxation. Int J Appl Glass Sci. 2022;13:338–46.

48. Phillips JC. Kohlrausch explained: the solution to a problem that is 150 years old. J Stat Phys. 1994;77(3):945–7.

49. Phillips JC. Stretched exponential relaxation in molecular and electronic glasses. Rep Prog Phys. 1996;59(9):1133.

50. Potuzak M, Welch RC, Mauro JC. Topological origin of stretched exponential relaxation in glass. J Chem Phys. 2011;135(21):214502.

51. Welch RC, Smith JR, Potuzak M, Guo X, Bowden BF, Kiczenski TJ, et al. Dynamics of glass relaxation at room temperature. Phys Rev Lett. 2013;110(26):265901.

52. Hara M, Suetoshi S. Density change of glass in transformation range. Report ofthe Research Laboratory, Asahi Glass Co. 1955;5:126–35.

53. Bradtmüller H, Gaddam A, Eckert H, Zanotto ED. Structural rearrangements during sub-Tg relaxation and nucleation in lithium disilicate glass revealed by a solid-state NMR and MD strategy. Acta Mater. 2022;240:118318.

SUPPORTING INFORMATION

Additional supporting information can be found online in the Supporting Information section at the end of this article.